THREE-DIMENSIONAL FINITE ELEMENT MODELING OF DILATED HUMAN ASCENDING AORTA

Ajay Bohra[1], Thoralf M. Sundt[3], and Ruth J. Okamoto[1,2]
Departments of [1]Mechanical Engineering and [2]Biomedical Engineering
Washington University
St. Louis, MO
[3]Division of Cardiovascular Surgery, Mayo Clinic
Rochester, MN

ABSTRACT

A dilated ascending aorta or aortic root is susceptible to fatal aortic dissection or rupture. This risk may be attributed to increased circumferential stresses due to an increase in aortic lumen diameter. However, the effect of complex geometry on wall stresses in the dilated ascending aorta is not well understood.

In this study, we combined pre-operative MRI data and measured mechanical properties of excised tissue to create a patient-specific three-dimensional finite element (FE) model of a dilated ascending aorta. Pressure loading conditions were applied using the brachial cuff pressure for the patient and physiologic boundary conditions were prescribed.

The model-predicted maximum circumferential stresses occurred distal to the maximum diameter on the inner curvature of the aorta (left posterior wall). Maximum axial stresses occurred on the outer curvature (right anterior wall) near the proximal end of the aorta. The spatial variations in the magnitude of stress components suggest that the complex three-dimensional shape of dilated ascending aorta may be important in determining the risk of rupture.

METHODS

Informed consent was obtained from a 55-year-old male with a dilated ascending aorta undergoing elective graft replacement of the ascending aorta. A pre-operative magnetic resonance imaging (MRI) scan was used to obtain FE model geometry and non-linear elastic properties were obtained from planar biaxial testing of an aortic tissue specimen removed from the patient during surgery (Okamoto et al. 2002).

Model Geometry

An MRI scan was carried out one day before surgery using a 1.5T whole body scanner (ACS-NT15, Philips Medical Systems). Brachial cuff pressure was monitored periodically during the scan. After locating the position of the aorta, multiple axial cross-sections were obtained with a sagittal oblique survey. Transverse cine scans were used to determine the transverse dimensions of the aorta at different positions along its axis. The contours of multiple sagittal oblique and transverse images were digitized using MATLAB, transformed to 3-D coordinates, and combined into a single data set. A smooth surface was created from this data using a surface-fitting program (Grimm et al. 2002).

This surface represents the aortic lumen under physiologic loading. In order to generate unloaded geometry, we fit the central axis of aorta to a cubic 3-D spline and determined the radius at 22 axial positions. We then divided the length of each spline segment by an initial axial scaling factor of 1.2, based on measurements of axial retraction made by Learoyd and Taylor (1966). We divided the radius at each axial position by an initial radial scaling factor of 1.5, estimated using a cylindrical model (Peterson and Okamoto 2000). We used these unloaded model dimensions and a uniform wall thickness of 2.57 mm that was measured from the biaxial test specimen to generate a 3-D solid model (SolidEdge v9, EDS Inc.). The unloaded model geometry was adjusted iteratively by changing the axial and radial scaling factors as explained below.

The solid model was meshed with 80 axial, 48 circumferential and 4 radial elements using TrueGrid v 2.1.5 (XYZ Scientific, Inc.) to create a mesh with 15360 eight-noded hexahedral elements.

Material Properties

The experimental data obtained from biaxial testing was fit to an incompressible, isotropic and non-linear strain energy function, W:

$$W = c_1 (I_1 - 3) + c_2 (I_1 - 3)^2 + c_3 (I_1 - 3)^3 \qquad (1)$$

where, c_1= 20.060 kPa, c_2=0.216 kPa, c_3 = 9.433 kPa are the coefficients obtained from fitting the biaxial test data and I_1 is the first invariant of the left Cauchy-Green deformation tensor. The function W was modified from the form proposed by Raghavan and Vorp (2000) for aneurysmal abdominal aorta by the addition of a cubic term to account for the greater non-linearity of dilated ascending aortic tissue.

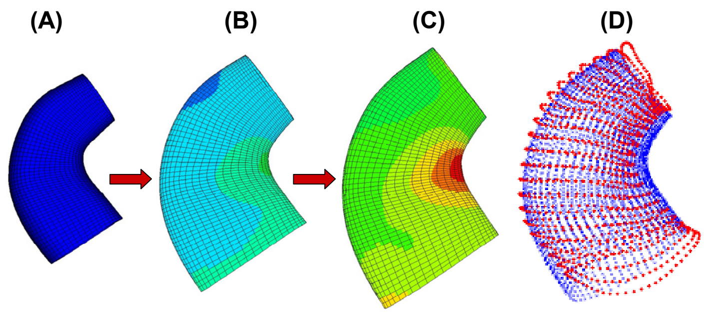

Figure 1. Model solution at (A) unloaded, (B) diastolic and (C) systolic loading, (D) Smoothed MRI data (red) superimposed on systolic solution (blue). Contours in (B) and (C) show mid-wall circumferential Cauchy stress components.

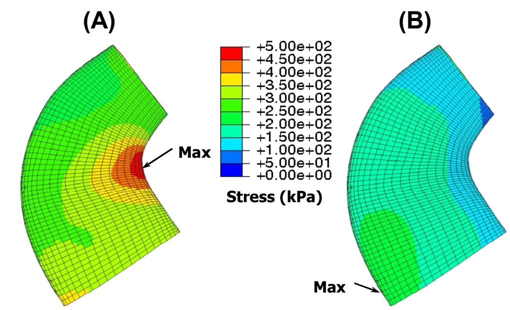

Figure 2. Distribution of model-predicted mid-wall circumferential (A) and axial (B) Cauchy stress components at systolic loading.Arrows indicate locations of maximum stress.

Iterative Model Solution

The model was solved using ABAQUS 6.2 (HKS, Inc.) with 8-noded incompressible hyperelastic hexahedral elements (C3D8RH). Loads and boundary conditions were applied using local cylindrical coordinate systems. First, the patient's diastolic brachial cuff pressure (10.27 kPa, 77 mm Hg) was applied to the inner surface of the model and axial displacements were applied to the proximal and distal ends. Next, the pressure was increased to the patient's systolic pressure (18 kPa, 135 mm Hg). The aorta moves significantly in the axial direction during the cardiac cycle (Kozerke et al. 1999). We accounted for this physiologic motion by increasing the axial displacement when solving the model with systolic pressure.

Since our model did not include the aortic root, we estimated the axial reaction forces on the proximal end of the ascending aorta during diastolic and systolic loading using a simplified model of the aortic sinuses and aortic valve annulus.

After initial FE model solution, we computed the axial reaction forces at the proximal end and compared them to our estimates of 20 N and 35 N at diastolic and systolic loading respectively. The model was solved iteratively by adjusting the axial scaling factor until the sum of reaction forces at the bottom end were greater than the estimates. The radial scaling factor was simultaneously adjusted until the smoothed MRI data lay between the systolic and the diastolic solution.

RESULTS

Using axial and radial scaling factors of 1.25 and 1.65 respectively, we were able to match the deformed model shape to the smoothed MRI data (Figure 1) and the estimated reaction forces. The model-predicted lumen radii varied axially from 15-24 mm and 16-26 mm at diastolic and systolic loading respectively.

Figure 2 shows the model-predicted circumferential and axial mid-wall Cauchy stress distributions at systolic loading. The spatial distribution of the circumferential and axial strains was similar to the corresponding stresses. The maximum mid-wall circumferential stress of 483 kPa and corresponding Green's strain of 1.09 occurred on the inner curvature (left posterior). The maximum mid-wall axial stress of 218 kPa and corresponding Green's strain of 0.40 occurred near the proximal end of the outer curvature (right anterior). The magnitudes of the maximum diastolic mid-wall stresses (220 kPa circ., 92 kPa axial) were lower but the locations were similar to systolic loading.

DISCUSSION

The circumferential and axial mid-wall stress distributions predicted by our model show that the curvature of dilated ascending aorta causes substantial variations in stress component magnitudes and may be important in determining the risk of rupture or dissection.

Our model uses patient-specific geometry and elastic properties. We have shown previously (Okamoto et al. 2002) that elastic properties of dilated ascending aorta vary with age. The elastic properties influence the scaling factors used to determine the final unloaded geometry in the iterative solution method. By using patient-specific properties, we can reduce errors introduced by scaling. Ideally, we would measure the unloaded dimensions of the entire ascending aorta to create the unloaded geometry. In practice, only a segment of the aorta is excised during surgery. The measured radius of a ring from this patient's excised aorta (1.45 cm) matched the unloaded model radius near its proximal end, indicating that our radial scaling factor was reasonable.

We have also previously found that the elastic properties of the ascending aorta are moderately anisotropic (Okamoto et al. 2002). In this model, we used an isotropic constitutive relation to simplify implementation in ABAQUS. The isotropic relation fit the biaxial test data for this patient reasonably well but slightly underestimated the experimentally measured circumferential stresses. The measured opening angle of the excised aortic ring was 250°, indicating the presence of circumferential residual stress that was not accounted for in this model. Hence we examined mid-wall stresses, which are relatively insensitive to opening angle when homogeneous material properties are assumed (Peterson and Okamoto 2000).

ACKNOWLEDGEMENTS

This research was funded by the Whitaker Foundation. We thank Dr. Cindy Grimm for her assistance with the MRI data fitting.

REFERENCES

Grimm CM, Crisco JJ, Laidlaw DH, 2002, "Fitting manifold surfaces to three-dimensional point clouds." *J Biomech Eng*, 124: 136-40.

Kozerke S, Scheidegger MB, Pedersen EM, Boesiger P, 1999, "Heart motion adapted cine phase-contrast flow measurements through the aortic valve." *Magn Reson Med*, 42: 970-8.

Learoyd BM, Taylor MG, 1966, "Alterations with age in the viscoelastic properties of human arterial walls." *Circ Res*, 18: 278-92.

Okamoto RJ, Wagenseil JE, DeLong WD, Peterson SJ, Kouchoukos NT, Sundt TM, 2002, "Mechanical Properties of Dilated Human Ascending Aorta." *Ann Biomed Eng*, 30: 624-635.

Peterson SJ, Okamoto RJ, 2000, "Effect of residual stress and heterogeneity on the stress distribution in the arterial wall." *J Biomech Eng*, 122: 454-456.

Raghavan ML, Vorp DA, 2000, "Toward a biomechanical tool to evaluate rupture potential of abdominal aortic aneurysm: identification of a finite strain constitutive model and evaluation of its applicability." *J Biomech*, 33(4), 475-82.